ZnO Nanorod-Based Ultraviolet Photodetector Prepared on Patterned Sapphire Substrates

Fang-Hsing Wang, *Member, IEEE*, and Chih-En Tsai

***Abstract*—A patterned sapphire substrate with a submicron hole array structure was used to fabricate ZnO nanorod (NR) array by low-temperature hydrothermal method. A ZnO seed layer was spin-coated using sol-gel process and then etched to form separated seed islands. Different concentrations of zinc acetate in the hydrothermal solution were performed for ZnO NR synthesis to investigate ultraviolet (UV) photo-response properties. The ZnO NRs synthesized on the patterned substrates were oriented at various inclined angles. The diameter of the NRs increased and their surface-to-volume ratio decreased as the concentrations of zinc acetate increased from 0.01 to 0.04 M. X-ray diffraction and photoluminescence analyses showed that the NRs synthesized at a higher zinc acetate concentration had better crystal quality and fewer defects. The current–voltage characteristics of the ZnO NR-based metal-semiconductor-metal photodetectors exhibited a linear relationship, suggesting an Ohmic contact between NRs and Al electrodes. The UV response, defined by the resistance ratio (R_{dark}/R_{UV}), of the photodetectors increased with the decreasing zinc acetate concentration from 0.04 to 0.01 M. Compared to traditional vertically aligned NR array on plain substrates, the proposed ZnO NR-based photodetector on the patterned substrates achieved improved UV responses, and the average increment for samples of 0.01–0.04 M was 145%.**

***Index Terms*—ZnO nanorod, photodetectors, ultraviolet, nanotechnology, patterned substrate.**

I. Introduction

ULTRAVIOLET (UV) photodetectors (PDs) have attracted increasing attention for last decade because of their wide applications in advanced communications, flame detection, air purification, ozone sensing and leak detection. UV photodetectors can be made based on wide band-gap semiconductor materials such as ZnO, GaN, SiC, SnO_2 and diamond [1]–[3]. Among these materials, ZnO possesses certain unique properties, such as a direct band gap (3.37 eV), large exciton binding energy (60 meV), high thermal and chemical stability, transparence, and wide electrical conductivity range, and has become promising materials in applications of optoelectronic devices and sensors [4]. UV PDs come out based on the bulk, thin film or nanostructure of the wide band-gap semiconductor materials. In general, the nanostructure materials have a higher photo responsivity because of scaling down of effective conductive channel and large surface to volume ratio. Especially, one-dimensional (1-D) nanostructures have become a highlighted research topic in fabricating electronic, optoelectronic, electrochemical, and electromechanical devices with nanoscale dimensions because of their special shapes, compositions, and chemical, and physical properties [5]. ZnO has many variety of different nanostructures, including nanorods, nanowires, nanobelts, nanocombs, nanorings, nanosprings, etc. Among them, 1-D ZnO nanorods (NRs) prepared by hydrothermal reaction have been widely studied because of advantages such as low cost and simple process [6]–[12]. Kim *et al.* tailored the surface area of ZnO nanorods by using different seed layers and precursor concentrations to improve sensing performance [8]. Chuang *et al.* developed a density-controlled and seedless growth method for laterally bridged ZnO nanorods as a metal–semiconductor–metal photodetector [9]. Their results indicated that highly dense lateral ZnO nanorod-based PDs achieved a higher responsivity than that with vertically aligned NRs.

In this study, we fabricated metal–semiconductor–metal (MSM) ZnO nanorod-based UV PDs on a patterned concave seeded substrates. The special seed layer was deposited on a sapphire substrate with a sub-micron honeycomb hole array structure using sol-gel spin-coating method. The UV response were investigated particularly as a function of surface-to-volume ratio of ZnO nanorods, which was tailored by the use of the patterned seed layer and/or by changing the concentration of the precursors in the hydrothermal growth solution.

II. Experiments

Fig. 1 displays the schematic flowchart of this experiment. The experimental procedures for two types of substrates were: (a) devices on flat glass or Si substrates: (1) cleaning substrates, (2) spin coating ZnO seed layers by sol-gel method and then annealing in Ar ambient at 500 °C for 1 h, (3) growing ZnO nanorod arrays, (4) depositing aluminum interdigitated electrodes, and (b) devices on patterned sapphire substrates: (1) cleaning substrate, (2) depositing ZnO seed layers and then annealing in Ar ambient at 500 °C for 1 h, (3) etching the seed layers to form separate ZnO films by a dilute HCl solution ($HCl:H_2O = 1:1000$) for 70 s, (4) growing ZnO nanorod arrays, (5) depositing aluminum interdigitated electrodes. Fig. 2 exhibits the plan-view SEM image of the patterned sapphire substrate with a sub-micron hole array, which were brought from Shun-Hua Technology Inc. and were fabricated via nanoimprint and etch method. The inset displays its cross sectional view. The hole pitch, height, and bottom diameter were about 1.5, 0.5, and 0.3 μm, respectively.

Manuscript received June 1, 2016; revised October 11, 2016; accepted November 7, 2016. This work was supported in part by the Ministry of Science and Technology of Taiwan under Grant MOST 103-2221-E-005-040-MY2.

The authors are with the Department of Electrical Engineering and Graduate Institute of Optoelectronic Engineering, National Chung Hsing University, Taichung 402, Taiwan, R.O.C. (e-mail: fansen@dragon.nchu.edu.tw; tsaichihen@gmail.com).

Color versions of one or more of the figures in this paper are available online at http://ieeexplore.ieee.org.

Digital Object Identifier 10.1109/JSTQE.2016.2630839

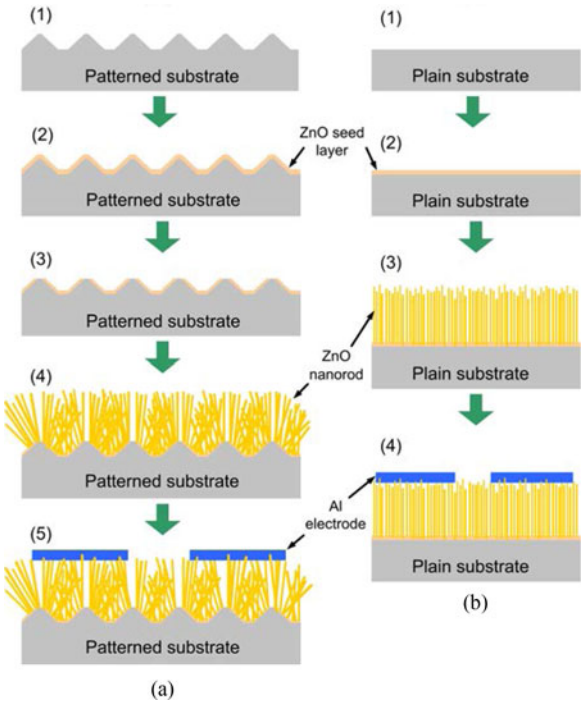

Fig. 1. Schematic flowchart of this experiment. The experimental procedure for the two types of devices: (a) PDs grown on patterned sapphire substrates, (b) PDs grown on plain Si (or glass) substrates.

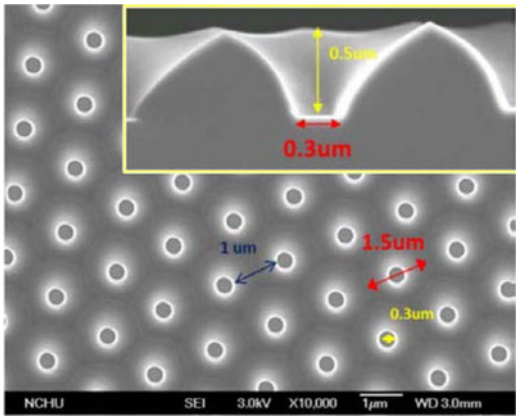

Fig. 2. Plan-view SEM image of the patterned sapphire substrate with a submicron hole array. The inset displays its cross sectional view.

The ZnO nanorod arrays were synthesized by hydrothermal method on seeded Corning eagle XG glass and patterned sapphire substrates. First, substrates were cleaned by supersonic bath in deionized water, acetone, and isopropyl alcohol sequentially. Second ZnO seed layers were deposited by sol–gel spin coating method. Then the ZnO seed layer on sapphire was etched by dilute hydrochloric acid to produce a patterned ZnO seed layer array. The source solutions for ZnO nanorods growth were prepared with the precursors, zinc acetate dehydrate $Zn(C_2H_3O_2)_2{\cdot}2H_2O$ and Hexamethylenetetramine (HMTA) $C_6H_{12}N_4$ as modifying agent in stoichiometric proportions dissolving in de-ionized water. The concentrations of

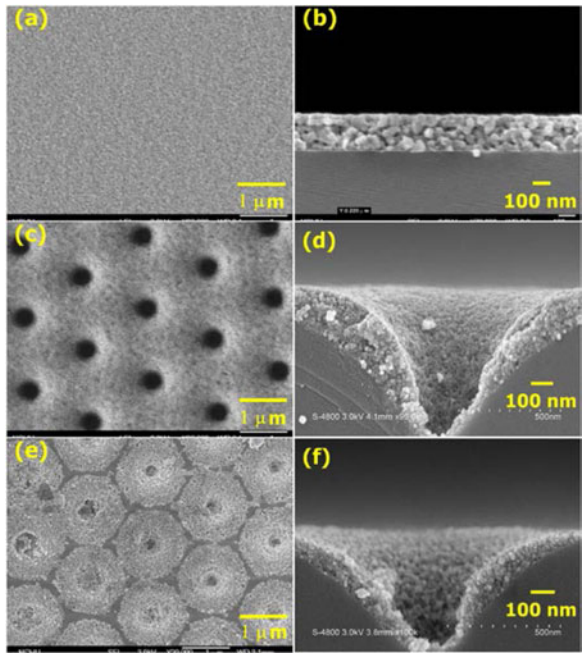

Fig. 3. Plan-view and cross-section FE-SEM images of the ZnO seed layer grown on different substrates: (a), (b) plane substrate, (c), (d) patterned sapphire substrate before wet etching, and (e), (f) patterned sapphire substrate after wet etching.

zinc acetate solution (0.01–0.04 M) with the growth time of 60 min were performed to grow ZnO nanorods.

The X-ray diffraction (XRD, PANalytical) with Cu–Kα radiation ($\lambda = 1.54056$ Å, θ–2θ scan mode) was used to characterize structural and crystallographic properties of the ZnO nanorods. Surface morphologies and size distribution of the ZnO nanorods were characterized by a field-emission scanning electron microscope (FE-SEM, JEOL, JSM–6700F). Photoluminescence (PL) spectroscopy (Horiba, iHR550) was employed at room temperature using a 325 nm He–Cd laser for the investigation of optical emission properties.

Finally, Al interdigitated electrodes with a thickness of 350 nm were deposited on the ZnO nanorod array using thermal evaporation to form metal-semiconductor-metal (MSM) photodetectors (PDs). The dark/photo currents were determined using a Keithley 2400 source meter interfaced with a computer under illumination from a 365 nm UV LED at RT in ambient atmosphere.

III. Results and Discussion

A. Growth of ZnO Nanorod Array

Fig. 3 shows plan-view and cross-section FE-SEM images of the ZnO seed layer grown on different substrates: (a, b) glass, (c, d) sapphire before wet etching, and (e, f) sapphire after wet etching. From the Fig. 3(a), the thickness of the ZnO seed layer deposited by sol-gel method was about 220 nm, and their surface particle size was about 30 nm. For the patterned sapphire substrates, we observed that the continuous seed layer on the concave surface (see Fig. 3(c)) had been separated into

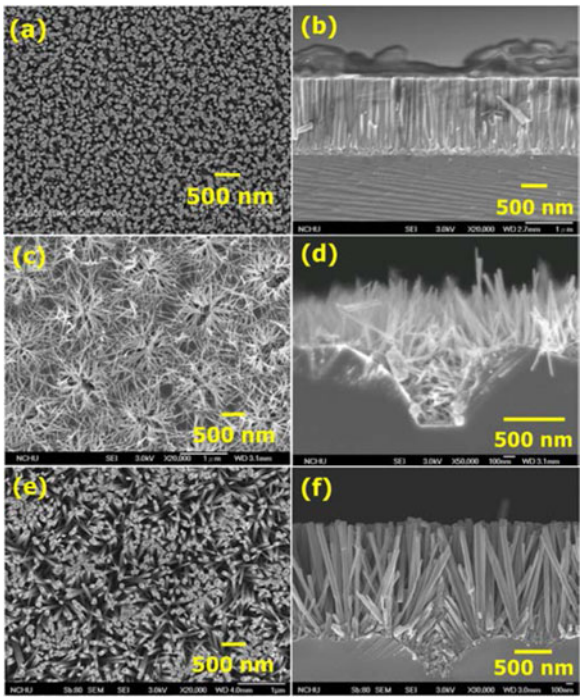

Fig. 4. Plan-view and cross-section FE-SEM images of the ZnO nanorods: (a), (b) 0.01 M grown on plain Si substrates, (c), (d) 0.01 M grown on patterned sapphire substrates, (e), (f) 0.03 M grown on patterned sapphire substrates.

TABLE I
STRUCTURES OF ZNO NRS GROWN ON SI SUBSTRATES WITH DIFFERENT CONCENTRATION OF ZINC ACETATE

Concentration of zinc acetate (M)	0.01	0.02	0.03	0.04
Diameter (nm)	50	60	95	150
Length (nm)	1600	1700	1650	1630
Density of ZnO NRs (μm^{-2})	100	110	85	40
Total surface area of ZnO NRs on 1 μm^2 seed layer (μm^2)	25.32	35.54	42.44	31.41
Total volume of ZnO NRs on 1 μm^2 seed layer (μm^2)	0.31	0.53	0.99	1.15
Surface-to-volume ratio	81.7	67.1	42.9	27.3

many independent seed islands in each comb-like hole after wet etching (see Fig. 3(e)).

Fig. 4(a)–(f) displays plan-view and cross-section FE-SEM images of ZnO nanorod array grown on different substrates. The typical vertically well-aligned ZnO nanorod array can be found on plain seeded substrates, as Fig. 4(a) and 4(b) shows. However, on the patterned substrate with a hole array, growth orientation of ZnO nanorods depended on the seed pattern and surface morphology of the substrate. Some of nanorods exhibited obliquely or laterally aligned structure instead of vertical ones (see Fig. 4 (c)–(f)). Besides, as comparing the nanorods grown with different concentrations of the precursor, we found that the stronger precursor concentration, the thicker and longer nanorods were. The estimated structural parameters of ZnO nanorods grown on plane Si substrates and patterned sapphire substrates with different concentrations of zinc acetate with growth time of 60 min were listed in Table I and Table II.

TABLE II
STRUCTURES OF ZNO NRS GROWN ON SAPPHIRE SUBSTRATES WITH DIFFERENT CONCENTRATION OF ZINC ACETATE

Concentration of zinc acetate (M)	0.01	0.02	0.03	0.04
Diameter (nm)	30	50	90	140
Length (nm)	900	1650	1700	1250
Density of ZnO NRs (μm^{-2})	105	60	65	50
Total surface area of ZnO NRs on 1 μm^2 seed layer (μm^2)	7.99	15.66	31.64	28.24
Total volume of ZnO NRs on 1 μm^2 seed layer (μm^2)	0.06	0.19	0.70	0.96
Surface-to-volume ratio	133.2	82.4	45.2	29.4

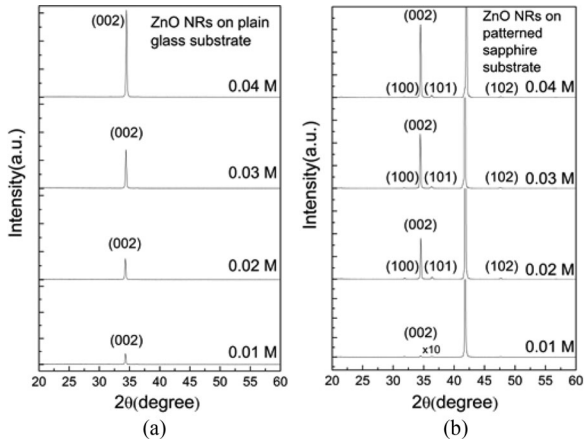

Fig. 5. $\theta-2\theta$ XRD patterns of ZnO nanorods prepared on (a) plain glass substrates and (b) patterned sapphire substrates as a function of zinc acetate concentration.

The diameter and total volume of ZnO nanorods both increased monotonically with the increase of the concentration of zinc acetate regardless of substrate type. The total surface area of ZnO nanorods increased and then decreased with the concentration of zinc acetate, and the maximum surface area was found with zinc acetate solution of 0.03 M. In comparison, the ZnO nanorods grown on the plain substrate had larger diameters and the total surface area than the other. It may be due the better crystal quality of the seed layer on the plain substrate because of without undergoing the etch process. The surface-to-volume ratio decreased with the increasing concentration of zinc acetate for both types of samples, and it was worth noting that the largest ratio (133.2) was achieved for 0.01 M on the patterned sapphire substrate.

Fig. 5 presents θ–2θ XRD patterns of ZnO nanorods as a function of concentration of zinc acetate in the hydrothermal solution. As seen in Fig. 5(a) and (b), all the ZnO nanorods exhibited polycrystalline nature with a highly (002) preferred orientation along the c-axis, indicating a typical wurtzite structure. The peak intensity increased as the concentration of zinc acetate increased, suggesting that the (002) peak intensity increased with the increase of the total volume of ZnO NRs. Compared to the ZnO nanorods on the patterned sapphire substrate, nanorods on the plain substrate possessed higher (002) peak intensity, revealing larger volume and better crystallinity. This

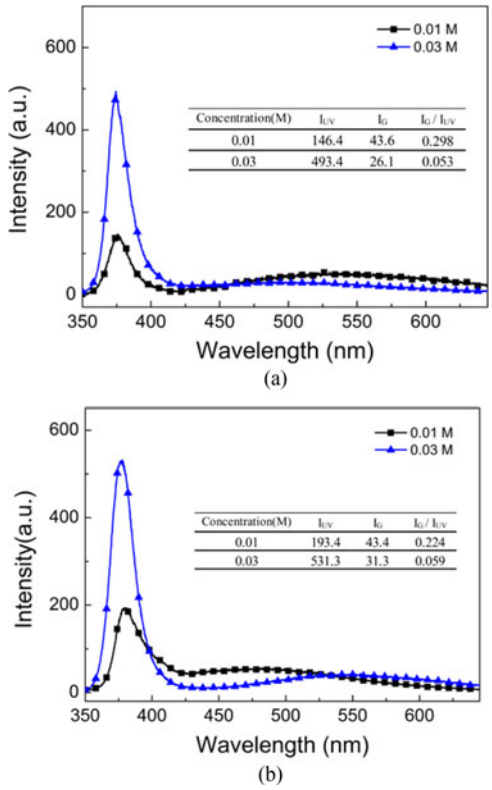

Fig. 6. Photoluminescence spectra of ZnO nanorods grown on (a) plain Si substrates and (b) patterned sapphire substrates.

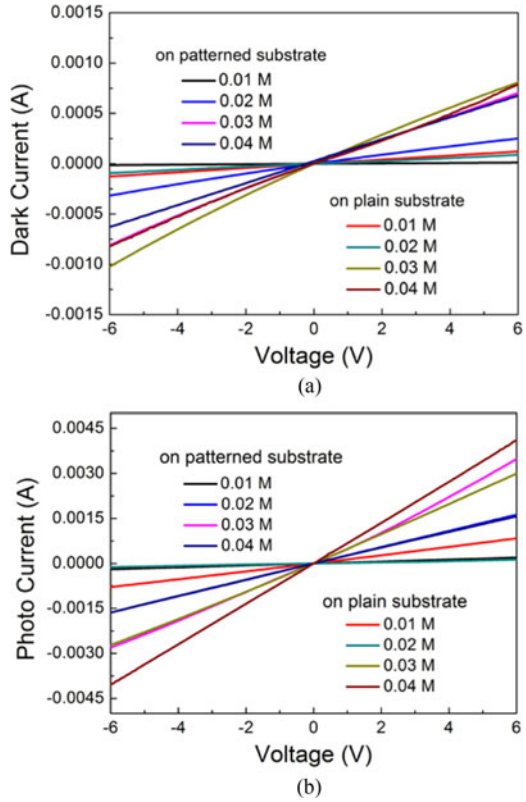

Fig. 7. (a) Dark and (b) photo currents of MSM ZnO NR PDs as a function of voltage for different concentrations and substrates.

result is consistent with the findings in the FE-SEM observation (Fig. 4).

Photoluminescence (PL) spectra of ZnO nanorods grown on different substrates are shown in Fig. 6. All samples exhibited two emission bands. The sharp UV emission band centered at around 374.4 nm corresponded to the near-band-edge emission and free-exciton peak of ZnO [13]. The broad green emission bands in the visible region were located at around 460–570 nm and were referred to as the intrinsic defects (e.g., oxygen vacancy and zinc interstitials) and crystal defects (e.g., luminescent centers) in the ZnO [14]–[16]. The insets list the intensities of the UV emission peak (I_{UV}) and the green emission band (I_G), as well as ratios of I_G/I_{UV}. Clearly, the NRs prepared with the precursor concentration of 0.03 M show enhanced UV emission and weakened green emission compared with those using 0.01 M regardless of substrate morphology. This is consistent with the results reported by Yang *et al.*, in which they found that the green emission relative to the UV emission increased as the nanowire diameter decreased [17]. The intensity ratio between green emission and UV emission bands (I_G/I_{UV}), which generally indicates the relative defect amount in ZnO, was smaller for the 0.03 M samples, revealing the less surface defects and higher crystal quality of the developed ZnO NRs in this condition [9].

B. Characteristics of UV Photodetectors

The MSM UV PDs were fabricated by evaporating Al interdigitated electrodes on ZnO nanorod arrays. Fig. 7 show I–V characteristics of the MSM PDs in dark and under UV illumination for different substrates. The observed highly linear relationship in the I–V characteristics demonstrated a good Ohmic contact property at the ZnO NRs and Al electrodes interface regardless of illumination and substrate type. Since the electron affinity of ZnO ($\chi_{ZnO} = 4.35$ eV) is higher than the work function of Al ($\Phi_{Al} = 4.25$ eV), an Ohmic contact would be expected to form as Al electrodes are deposited on ZnO nanorods. At 5.0 V voltage bias, the dark and photo currents of the 0.01 M device on the patterned substrate were 9.65 and 162 μA. The dark current corresponds to the leakage current of the MSM PDs. In dark ambient, oxygen molecules absorb on ZnO nanorod surface and capture free electrons, and a depletion region is formed near the surface, leading to a low current. Upon UV illumination, electron–hole pairs are photo-generated, and then holes are readily trapped at the surface or combined with negatively charged absorbed oxygen ions, leaving behind electrons in the nanorods that transport to anodes and contribute to the high photocurrent. It is clear that the ZnO nanorod-based PDs is highly sensitive to UV light, and the photocurrent increases by approximate 16 times of magnitude compared to the dark current. The dark and photo resistances could be calculated as 518 and 30.9 kΩ, respectively for this device. Fig. 8

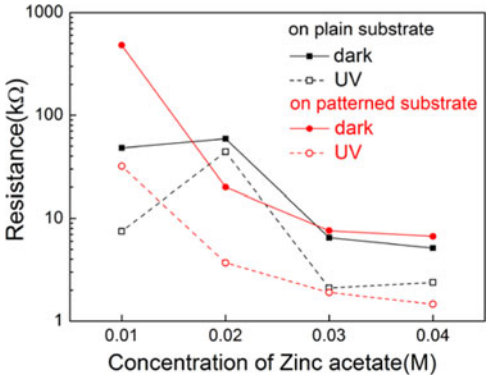

Fig. 8. Dark/UV resistances of MSM ZnO NR PDs as a function of zinc acetate concentration for different substrates.

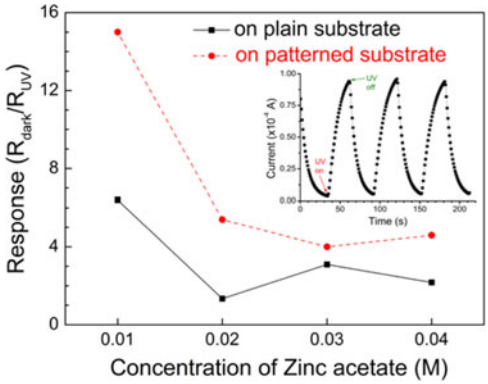

Fig. 9. Response ($\mathrm{R_{dark}}/\mathrm{R_{UV}}$) of MSM ZnO NR PDs as a function of zinc acetate concentration for different substrates. The inset shows the current–time relationship for three on/off illumination cycles.

presents calculated dark and UV resistances of PDs as a function of zinc acetate concentration. The resistance of PDs gradually decreased as the concentration of zinc acetate increased because of the thick nanorods and the improved crystallinity at the high concentration. The maximum of resistance occurred at the 0.02 M and 0.01 M for the plain and patterned substrates, respectively. On the other hand, the resistances of all PDs decreased under illumination. It may be attributed to fast band-to-band recombination and/or hole-trapping effect based on the existence of chemisorbed oxygen molecules at surfaces [18], [19].

Fig. 9 displays UV response of PDs as a function of zinc acetate concentration for different substrates. The response is calculated by $\mathrm{R_{dark}}$ dividing $\mathrm{R_{UV}}$. The inset shows the current–time relationship for three on/off illumination cycles, which demonstrates good stability of the fabricated PDs. From the Fig. 9, we observed that the UV response decreased with the increase of the zinc acetate concentration for both types of substrates. The obtained highest responses were 15.0 and 6.4 for PDs grown on the plain and patterned substrates, respectively. It is of interest to note that the PDs on the patterned substrates achieved higher UV response than those on the plain substrates, and the average increment for all the samples with zinc acetate concentration of 0.01–0.04 M was 145%. This result suggests that the high response is strongly related to the surface-to-volume ratio of ZnO NRs (as Tables I and II list). The large surface area of nanorods enhances hole-trapping effect through chemisorbed oxygen molecules at surfaces. Additionally, the obliquely and laterally aligned nanorods on the patterned substrates also improve the internal photoconductive gain, thus raising the UV response, in accordance with the works of Chuang *et al.* [9] The remarkably enhanced UV response suggests that the proposed ZnO nanorods fabricated on the patterned substrate with a hole array provides a novel method for future applications of high-performance UV photodetector.

IV. Conclusion

ZnO nanorod array based UV photodetectors have been fabricated on patterned sapphire substrates with a sub-micron hole array structure by low-temperature hydrothermal method. The aspect ratio, density, and surface-to-volume ratio of NRs could be controlled by adjusting concentration of precursor (zinc acetate). The inclined angle of NRs is dependent on morphology of substrate (i.e., plain or patterned substrate). At the precursor concentration of 0.01 M, the developed ZnO NR array based UV PD achieved the highest UV response ($\mathrm{R_{dark}}/\mathrm{R_{UV}}$) of 15.0 on the patterned sapphire substrate, which was 2.3 times greater than that prepared on the plain substrate. The effective improvement on UV response makes the developed ZnO NR-based devices for low-cost and high-performance UV PD applications.

References

[1] H. Zhu *et al.*, "High spectrum selectivity ultraviolet photodetector fabricated from an n-ZnO/p-GaN heterojunction," *J. Phys. Chem. C*, vol. 112, no. 51, pp. 20546–20548, Nov. 2008.

[2] W. C. Lien *et al.*, "4H-SiC metal-semiconductor-metal ultraviolet photodetectors in operation of 450 °C," *IEEE Electron Device Lett.*, vol. 33, no. 11, pp. 1586–1588, Oct. 2012.

[3] S. Almavivaa *et al.*, "Extreme UV photodetectors based on CVD single crystal diamond in a p-type/intrinsic/metal configuration," *Diamond Related Mater.*, vol. 18, no. 1, pp. 101–105, Jan. 2009.

[4] Z. L. Wang, "Characterizing the structure and properties of individual wire-like nanoentities," *Adv. Mater.* vol. 12, pp. 1295–1298, 2000.

[5] T. Zhai *et al.*, "A comprehensive review of one-dimensional metal-oxide nanostructure photodetectors," *Sensors*, vol. 9, no. 8, pp. 6504–6529, Aug. 2009.

[6] D. Barreca *et al.*, "1D ZnO nano-assemblies by Plasma-CVD as chemical sensors for flammable and toxic gases," *Sens. Actuat. B*, vol. 149, pp. 1–7, 2010.

[7] Z. Zhou, W. Peng, S. Ke, and H. Deng, "Tetrapod-shaped ZnO whisker and its composites," *J. Mater. Process. Technol.*, vol. 89, pp. 415–418, 1999.

[8] J. Y. Kim *et al.*, "Tailoring the surface area of ZnO nanorods for improved performance in glucose sensors," *Sens. Actuat. B*, vol. 192, pp. 216–220, 2014.

[9] M. Y. Chuang *et al.*, "Density-controlled and seedless growth of laterally bridged ZnO nanorod for UV photodetector applications," *Sens. Actuat. B*, vol. 202, pp. 810–819, 2014.

[10] B. A. Albissa, M.-A. AL-Akhras, and I. Obaidatc, "Ultraviolet photodetector based on ZnO nanorods grown on a flexible PDMS substrate," *Int. J. Environ. Anal. Chem.*, vol. 95, no. 4, pp. 339–348, Mar. 2015.

[11] W. Cheng, L. Tang, J. Xiang, R. Ji, and J. Zhao, "An extreme high-performance ultraviolet photovoltaic detector based on a ZnO nanorods/phenanthrene heterojunction," *RSC Adv.*, vol. 6, pp. 12076–12080, 2016.

[12] C. Tian *et al.*, "Performance enhancement of ZnO UV photodetectors by surface plasmons," *ACS Appl. Mater. Interfaces*, vol. 6, no. 3, pp. 2162–2166, Jan. 2014.

[13] Z. K. Tang, G. K. L. Wong, and P. Yu, "Room-temperature ultraviolet laser emission from self-assembled ZnO microcrystallite thin films," *Appl. Phys. Lett.*, vol. 72, pp. 3270–3272, 1998.
[14] B. Lin, Z. Fu, and Y. Jia, "Green luminescent center in undoped zinc oxide films deposited on silicon substrates," *Appl. Phys. Lett.*, vol. 79, pp. 943–945, 2001.
[15] T. Singh, D. K. Pandya, and R. Singh, "Surface plasmon enhanced bandgap emission of electrochemically grown ZnO nanorods using Au nanoparticles," *Thin Solid Films*, vol. 520, no. 14, pp. 4646–4649, May 2012.
[16] B. A. Albiss, M.-A. AL-Akhras, and I. Obaidat, "Ultraviolet photodetector based on ZnO nanorods grown on a flexible PDMS substrate," *Int. J. Environ. Anal. Chem.*, vol. 95, no. 4, pp. 339–348, 2015.
[17] P. Yang *et al.*, "Controlled growth of ZnO nanowires and their optical properties," *Adv. Funct. Mater.* vol. 12, no. 5, pp. 323–331, May 2002.
[18] J. D. Prades *et al.*, "The effects of electron-hole separation on the photoconductivity of individual metal oxide nanowires," *Nanotechnology,* vol. 19, 2008, Art. no. 465501.
[19] J. H. He, P. H. Chang, C. Y. Chen, and K. T. Tsai, "Electrical and optoelectronic characterization of a ZnO nanowire contacted by focused-ion-beam-deposited Pt," *Nanotechnology*, vol. 20, pp. 135701:1–135701:5, 2009.

Fang-Hsing Wang (M'14) was born in Taiwan, in 1968. He received the B.S. and Ph.D. degrees in electronic engineering from National Chiao-Tung University, Hsinchu, Taiwan, in 1991 and 1997, respectively.

He was employed by Unipac Optoelectronic Corporation from 1999–2001, where he researched and developed technologies of TFT-LCDs. During 2002–2003, he worked for Novatek Corporation to be an IC designer for display driving ICs. In 2003, he joined the faculty of National Chung-Hsing University, Taichung, Taiwan, as an Assistant Professor. Since 2011, he has been an Associate Professor in the Department of Electrical Engineering and Graduate Institute of Optoelectronic Engineering, National Chung-Hsing University, Taichung, Taiwan. He is the author of more than 110 articles and 22 inventions. His research interests include technologies of flat-panel displays and zinc oxide-based thin-films and devices.

Prof. Wang received the TACT International Conference Poster Paper Award in 2011.

Chih-En Tsai received the B.S. degree in electrical engineering from Yuan Ze University, Taoyuan, Taiwan, in 2012 and the M.S. degree in electrical engineering from National Chung Hsing University, Taichung, Taiwan, in 2015. His research interest includes the characteristics of ZnO nanorods, gas/UV light detectors, and the process and analysis of TCO films.